PROBABILITIES AND CHARACTERISTICS OF TSUNAMIGENIC UNDERWATER LANDSLIDES AND SLUMPS

Philip Watts

Applied Fluids Engineering, Private Mail Box #237, 5710 E. 7th Street, Long Beach, CA 90803, USA. E-mail: *phil.watts@appliedfluids.com.*

A review of the largest tsunamis this decade will reveal a significant percentage of events that probably involved tsunamigenic mass failure. Submarine mass failure includes underwater landslides, underwater slumps, and reef failure, most often triggered by a nearby earthquake. The differences between each type of mass failure event will be described, including center of mass motion and rates of deformation. Tsunami features such as period and amplitude depend primarily on the center of mass motion. A geological context derived from marine surveys is needed to identify the type of mass failure and pinpoint the size and location of a recent event. Mass failure tsunamis often arrive soon after generation, present a leading depression N-wave, and possess much larger than expected wave amplitude. Probability distributions of tsunami amplitudes generated by mass failure events are given for the first time. Earthquakes are invariably accompanied by mass failure events, although these may not be tsunamigenic. Probabilistic calculations of underwater landslides and slumps off of Southern California yield preliminary distributions of mass failure dimensions. Tsunami amplitude is calculated from accurate two-dimensional correlations based on numerical simulations of mass failure events. About half of all earthquakes do not experience significant tsunamis generated by mass failure. However, a finite probability exists for mass failure to generate tsunamis with amplitudes well in excess of 10 meters. The probabilities of nearshore and offshore earthquakes can be converted directly into tsunami hazards from submarine mass failure. Recent work on the Papua New Guinea event shows that large mass failure events can be detected seismically and possess distinct seismic characteristics. This enables tsunami warnings to be issued shortly after a large mass failure event, perhaps in time to mitigate its impact on coastal communities and infrastructure.

1) INTRODUCTION

Increased human coastal population and development coupled with devastating losses in recent history motivate tsunami hazard mitigation efforts. Tsunamis may be generated by volcanic eruptions, coseismic sea floor displacement, gas hydrate phase change, underwater landslides and slumps, and oceanic meteor strikes. Underwater landslide or slump generated tsunamis remain one of the least studied of these five mechanisms, in part because their occurrence is concealed and in part because of the complicated dynamics involved in failure, center of mass motion, and deformation. Underwater landslides and slumps also

pose difficulties for tsunami warning systems as they often occur on coastal margins near shorelines, can not be predicted as of yet, and may strike within minutes following a moderate earthquake. On the other hand, tsunamis generated by underwater landslides and slumps often cause limited damage outside of some range of influence. Scientists are currently unable to assess underwater landslide and slump hazards, predict their occurrence following a nearby earthquake, evaluate their tsunamigenic potential, and warn coastal communities of imminent danger. Underwater landslides and slumps pose a continuous threat to coastal economic activity, including valuable offshore structures and port facilities.

Coseismic displacement and mass failure constitute the two most common forms of tsunami generation. Coseismic displacement, or vertical seafloor deformation, occurs during most earthquakes and often generates tsunamis with longer wavelengths, longer periods, and a larger source area than those generated by mass failures (Hammack, 1973; Watts, 1998, 2000). Hence, coseismic displacement can produce transoceanic tsunamis, whereas mass failures produce tsunamis that decay rapidly away from the generation region, as if waves were eminating from a point source (Plafker *et al.*, 1969). Coseismic displacement generates tsunami amplitudes that correlate with earthquake magnitude (Hammack, 1973; Geist, 1998); submarine mass failures produce tsunamis with amplitudes limited only by the vertical extent of center of mass motion (Watts, 1998). Both mass failure center of mass motion and tsunami generation can surpass those of coseismic displacement by two orders of magnitude, posing a greater threat to coastal communities than previously recognized. Wave generation by submarine mass failure depends on at least four nondimensional geometric parameters -- length, width, thickness, and slope. The purpose of this work is to demonstrate that these quantities can be calculated for hypothetical earthquakes and thereby satisfy the urgent need to quantify mass failure tsunami hazards.

1.a Review of Recent Tsunamis

Historical records verify the tsunami hazards posed by submarine mass failure. Most tsunami damage and fatalities within Prince William Sound following the 1964 Good Friday, Alaskan earthquake resulted from local waves generated by submarine mass failure (Plafker *et al.*, 1969). Tsunamis generated by mass failure were larger in amplitude and arrived earlier than the transoceanic tsunami attributed to the M_W=9.2 earthquake (Plafker *et al.*, 1969). Since 1992, there have been twelve major local tsunamis: Nicaragua, 1992; Flores Island, Indonesia, 1992; Okushiri, Japan, 1993; East Java, Indonesia, 1994; Shikotan, South Kuril Islands, 1994; Mindoro, Philippines, 1994; Skagway, Alaska, 1994; Irian Jaya,

Indonesia, 1996; Chimbote, Peru, 1996; Kamchatka, Russia, 1997; Sissano, Papua New Guinea, 1998; and Izmit Bay, Turkey, 1999. The majority of these tsunamis demonstrated regions of peaked longshore runup distributions. For example, runup produced by the Flores Island tsunami showed a modest runup plateau punctuated by numerous large peaks that correlated with reef failure and subaerial landslides (Imamura and Gica, 1996). The Papua New Guinea tsunami has been the subject of extensive marine surveys to describe the suspected slump source (Tappin *et al.*, 1999). Five other events, Nicaragua, Mindoro, Skagway, Kamchatka, and Izmit Bay are known or suspected to have involved significant mass failure tsunami generation, with or without significant coseismic displacement. These events generated tsunami runup reaching 30 m above sea level, far surpassing most previous predictions of maximum tsunami amplitude for such moderate earthquakes and calling into question the preparedness of any coastal community for a similar event. It appears that tsunamigenic submarine mass failures accompany many nearshore earthquakes. We will attempt to predict the frequency of tsunamigenic mass failure off of Southern California below.

1.b Types of Submarine Mass Failure

Tsunamigenic underwater landslides and slumps involve the failure of a mass of sediment (or fill) that can range in length over more than six orders of magnitude, with larger events typically occurring less frequently (Prior and Coleman, 1979; Edgers and Karlsrud, 1982; Schwab *et al.*, 1993). Damaging tsunamis may result from the failure of sediment along steep fjords banks, near boundaries of submarine canyon systems, at active river deltas, along volcanic islands or ridges, or at submerged alluvial plains including continental margins (Hampton *et al.*, 1996). Terzaghi (1956) showed that underwater landslides and slumps can often be related to excess pore water pressures along (at least) the initial failure plane. Prior and Coleman (1979) attribute excess pore water pressure to low tides, artesian water flows, recent external loads, rapid sedimentation, seismic ground motions, construction induced vibrations, volcanic activity, vaporization of gas hydrates, wave action, or any combination of these or similar factors. Hampton *et al.* (1996) separate these factors into those that reduce effective sediment strength and those that increase sediment stress. Most tsunamigenic underwater landslides and slumps are triggered by local earthquakes.

Submarine mass failure is a broad term encompassing reef failure, rock slides, noncohesive landslides, and cohesive slumps. There are no clear definitions of these terms as rock may be significantly weathered or partially lithified, sand and silts may possess mild cohesion,

and biogenic muds often contain some concentration of silt. Instead, there is a spectrum of mass failure materials that each possess distinct modes of failure and subsequent behaviors. Any submerged geological structure can be expected to undergo some degree of submarine mass failure due to strong ground motion from a nearby earthquake (Tappin *et al.*, 1999). As such, all forms of submarine mass failure can be present at the same time. Given the ubiquity of mass failure, we are indeed fortunate that most events are not tsunamigenic on account of their small size or deep submergence. Here, the focus will be on two idealized forms of mass movement: noncohesive landslides and cohesive slumps. Underwater landslides are identified by translational failure while underwater slumps are defined to undergo rotational failure (Schwab *et al.*, 1993). Underwater landslides typically exhibit maximum thickness to initial length ratios of 0.5-2%; in contrast, underwater slumps often involve deep failure with maximum thickness to initial length ratios of 5-15% (Prior and Coleman, 1979; Turner and Schuster, 1996). Schwab *et al.* (1993) estimate that nearly half of all mass failures off of the continental United States appear to satisfy translational landsliding, while the other half appear to satisfy rotational slumping. The distinction is best made from the thickness to length ratio of the mass failure scar or sediment mass.

1.c Center of Mass Motions

Water wave amplitudes above an underwater landslide or slump scale with characteristics of center of mass motion (Watts, 1998, 2000). Moreover, numerical simulations need to reproduce an accurate initial acceleration before introducing and interpreting effects of landslide deformation and changing bathymetry. Both noncohesive landslides and cohesive slumps will be considered as semi-ellipses with a maximum thickness T measured from a major axis of total length b. Instead of studying geometrical differences, we will contrast the center of mass motions of submarine landslides and slumps. The frictionless motion of a noncohesional landslide is limited by fluid dynamic drag. By the time the landslide comes to rest within some oceanic deep, considerable deformation and spreading may have occurred. On the other hand, the rotation of a cohesive slump is retarded by significant basal friction that can keep fluid dynamic drag from reaching important scales. While a slump may not travel very far, it often breaks into distinct blocks that experience significant relative motion. The following analytical results provide convenient asymptotic limits for these two types of motion. Many real failure events are expected to move in a manner combining aspects of each analysis. As such, these results provide important information about the forces that produce mass failure center of mass motions.

Dobry *et al*. (1982) and Seed *et al*. (1988) show that sand and silt can experience an order of magnitude drop in shear strength during failure, thereby justifying neglect of Coulomb friction in center of mass motion. The solution of the approximate equation of motion becomes

$$s(t) = s_o \ln [\cosh (\frac{t}{t_o})] \tag{1}$$

which provides the landslide center of mass position along a straight incline as a function of time subject to the initial condition s(0)=0. Equ. (1) is a standard analytical solution of free bodies sliding down an incline subject to form drag at high Reynolds numbers (Watts, 1998; Pelinovsky and Poplavsky, 1996). The theoretical initial acceleration of a semi-ellipse landslide is approximately

$$a_o = \frac{(\gamma - 1) g \sin \theta}{\gamma + C_m} \tag{2}$$

where γ is the bulk specific density, g is the acceleration of gravity, θ is the incline angle, and the chosen added mass coefficient $C_m \approx 1$ is that of a circular cylinder (Sarpkaya and Isaacson, 1981). The landslide terminal velocity is approximately

$$u_t = \sqrt{\frac{\pi b (\gamma - 1) g \sin \theta}{2 C_d}} \tag{3}$$

where b is the landslide length along the incline, and the chosen drag coefficient $C_d \approx 1$ is also that of a circular cylinder. One may readily verify that the initial acceleration (2) and terminal velocity (3) are not sensitive functions of the dynamical coefficients C_m and C_d for landslides with specific density $\gamma \approx 1.85$. The characteristic distance s_o and characteristic time t_o of landslide motion

$$s_o = \frac{u_t^2}{a_o} \ , \ t_o = \frac{u_t}{a_o} \tag{4}$$

are derived directly from the differential equation of motion and are invertible functions of the initial acceleration and the terminal velocity. A unique characteristic distance and time of motion exist for each underwater landslide.

We model a slump as a rigid body moving along a circular arc subject to external moments from added mass, buoyancy, gravity, and shear stress along the failure plane. The critical state shear stress along the failure plane is assumed to remain constant during motion (Bardet, 1997). We invoke the small angle approximation and solve the linear differential equation of a damped pendulum. Multiplying the solution by the radius of curvature gives the slump center of mass position along the failure arc

$$s(t) = s_o \left[1 - \cos\left(\frac{t}{t_o}\right)\right] \tag{5}$$

where $s(0)=0$ and (5) remains valid for times $0<t/t_o<\pi$. The influence of quadratic fluid dynamic drag and angular nonlinearity on center of mass motion can be found from the exact solution given by Nayfeh and Mook (1979). The characteristic slump distance of motion is given by

$$s_o = \frac{R\,(\phi_f - \phi_i)}{2} = \frac{9\,R\,S_u}{4\,T\,g\,(\rho_b - \rho_o)} \tag{6}$$

where R is the radius of curvature, ϕ_i is the initial center of mass angle in radians, ϕ_f is the final center of mass angle in radians, S_u is the sediment shear strength, T is the maximum slump thickness, ρ_b is the bulk density of the slump, and ρ_o is the density of seawater. Equ. 6 can be utilized to estimate a mean shear strength S_u along the failure plane. For an underwater slump, s_o is simply the distance traveled by the center of mass. The characteristic time of motion is

$$t_o = \sqrt{\frac{g\,(\gamma - 1)}{R\,(\gamma + C_m)}} \tag{7}$$

in accordance with the period of pendular motion. For a slump, it is easier to construct the maximum velocity and initial acceleration

$$u_{max} = \frac{s_o}{t_o}\ ,\ a_o = \frac{s_o}{t_o^2} \tag{8}$$

from the characteristic distance and time of slump motion. Equs. (4) and (8) are seen to be reciprocal. This is a general feature of any accelerational motion characterized by one length scale and one time scale. This occurs whenever there is only one retarding force.

2) MASS FAILURE TSUNAMI GENERATION

Existing analyses of events such as the 1979 event at Nice, France by Seed *et al*. (1988) and the 1994 event at Skagway, Alaska by Cornforth and Lowell (1996) rely heavily on geotechnical parameters acquired following the landslides. Neither of these events involved mobilization of sediment by an earthquake. Lee and Edwards (1986) evaluate a simple earthquake-induced failure criterion against four underwater landslides with encouraging results. Housner (1985) describes the liquefaction of soils while Dobry *et al*. (1982) relate liquefaction to cyclic sediment loading during an earthquake. Morgenstern and Price (1965) present a general method for determining failure surfaces for a given soil strength distribution. Turner and Schuster (1996) discuss methods for estimating failure planes during an earthquake. We currently lack comparisons and sensitivity analyses of these different failure analyses. Regardless, we need and use such methods to predict the geometry of mass failure following a nearby earthquake.

2.a Marine Surveys

Underwater landslide motion is characterized by specific density γ, length along the incline b, and incline angle θ. These quantities can be estimated from bathymetry data acquired during a marine survey of suspected tsunami sources. Underwater slumps require a radius of curvature R, slump thickness T, and shear strength S_u to describe motion. These quantities require more sophisticated seismic reflection and core sampling tools. In either case, marine surveys conducted by experienced geologists are essential for understanding tsunamis generated by mass failure (e.g., Tappin *et al*., 1999). Knowledge of offshore structures, previous mass failure scars, sediment types, sedimentation rates, subsidence rates, and other geological features enable prediction of mass failure during or following a nearby earthquake. Motivation for tsunami hazard mitigation follows from accurate predictions of mass failure and tsunami amplitude given random earthquakes. For a specific earthquake, such knowledge enhances the accuracy of tsunami warnings, a critical feature of any warning system. The threat of tsunamis generated by mass failure promotes further reliance on marine geology and marine surveys in addition to seismic tools.

2.b Scaling of Tsunami Features

The scaling analyses of Watts (1998, 2000) provide a direct means of relating tsunami generation to submarine mass failure geometry and motion. The characteristic period of a

mass failure tsunami is given by t_o, the characteristic time of motion. The characteristic wavelength follows from

$$\lambda_o = t_o \sqrt{g\, d} \tag{9}$$

where d is the initial submergence at the middle of the landslide or slump. In terms of primitive variables, any near-field wave amplitude is a function of

$$\frac{\eta}{s_o \sin\theta} = f\left(\gamma, \frac{d}{b}, \frac{T}{b}, \theta, C_m, C_d\right) \tag{10}$$

where the values γ=1.85, C_m=1, and C_d=1 are fixed here for simplicity. One is free to choose any characteristic wave amplitude for which to construct the function (10). The maximum tsunami amplitude above the initial mass failure location is chosen here as a characteristic tsunami amplitude. Experience with a handful of case studies has shown that the maximum runup of local tsunamis has a value similar to the characteristic tsunami amplitude due to the compensating effects of tsunami propagation and shoaling. Most underwater landslides and slumps considered here will generate linear tsunamis that satisfy the linearity criteria

$$\frac{d}{b} \gg \frac{b}{g\, t_o^2} \;,\; \frac{d}{b} \gg \frac{s_o \sin\theta}{t_o \sqrt{g\, d}} \tag{11}$$

derived by Watts (1998). A submarine mass failure must be much wider than the local water depth and the local wavelength

$$w \gg d \;,\; w \gg t_o \sqrt{g\, d} \tag{12}$$

in order to generate roughly two-dimensional tsunamis that are only mildly affected by the third dimension. The criteria in (12) may be met by less than half of all tsunamigenic mass failures. The criteria in (12) are assumed to hold here and would need to be checked on a case by case basis.

2.c Approximate Tsunami Model

Grilli *et al*. (1989), Grilli and Svendsen (1990), and Grilli and Subramanya (1994, 1996) describe the development and validation of an efficient two-dimensional boundary element model of inviscid, irrotational free surface flows. The boundary element model features fully nonlinear boundary conditions and second order accurate updating of free surface position. Grilli and Watts (1999) applied the boundary element model to water waves generated by underwater landslides and performed a sensitivity analysis for one underwater landslide scenario. In this work, we employ the same model problem whereby an underwater landslide or slump is modeled as a semi-ellipse. The semi-ellipse has length b along the major axis which in turn rests on a straight incline with angle θ from horizontal. The semi-ellipse has a thickness T along half the minor axis and an initial vertical submergence d at the middle. We prescribe the landslide or slump center of mass motion along the incline and assume negligible deformation. Solutions of our two-dimensional model problem are based on exact velocity potential field equations and boundary conditions along a carefully discretized boundary. Our solutions extend the application of leading depression N-waves to tsunamis generated by underwater landslides and slumps (Tadepalli and Synolakis, 1994, 1996).

The model problem considered here consists of a semi-ellipse sliding down a straight incline with center of mass motion prescribed either by (1) or by (5). Numerical experiments are converted via (10) into predictive correlations of tsunami amplitude that are both accurate and simple analytical functions of nondimensional quantities. These correlations enable rapid case studies and inexpensive tsunami hazard mitigation. Following the form of (10), we find the remarkable result that, to within a 20% curve fitting error, the characteristic tsunami amplitude can be written

$$\eta = k\, s_o\, F(\sin\theta)\, G\left(\frac{T}{T_{ref}}\right) H\left(\frac{d}{d_{ref}}\right) \tag{13}$$

where k is a coefficient that depends on the type of mass failure (or center of mass motion), T_{ref} is a reference thickness, and d_{ref} is a reference depth, both chosen to be proportional to b sin θ. Equ. (13) is limited to events that satisfy (11) and (12). In the final form of the correlation, the reference values are replaced by their respective functions of b, θ, and R. For any given mass failure event, the accuracy of (13) depends on the semi-ellipse geometrical approximations inherent to the functions F, G, and H, as well as the dynamical approximation represented by s_o. The semi-ellipse considered here is likely a good approximation of most underwater landslides and slumps, whereas the solutions for center

of mass motion represent two separate extremes between which there are many possible variations. Hence, our lack of knowledge about mass failure center of mass motion limits the accuracy of any numerical simulation and of s_o in (13). Nevertheless, (13) provides a very rapid and inexpensive means to estimate tsunami amplitude and gauge the sensitivity of that amplitude on geometrical and dynamical quantities.

3) TSUNAMI AMPLITUDE DISTRIBUTION

A novel algorithm is developed to examine the probability distribution of tsunami amplitude when generated by submarine mass failure. The algorithm uses realistic probability distributions to span the parameter space of possible nearshore geologies encountered off of Southern California. The dependence of tsunami amplitude with respect to each geological input can thus be evaluated. The results given here are preliminary and subject to revision, especially since actual geological and sedimentary data are not used. Hence, we will forego a detailed analysis of model results in favor of the implications of selected results on tsunami hazard and warning. Uncertainty in the center of mass motions and probability distributions are reduced by considering the combined results of underwater landslide and slump calculations.

3.a Earthquake Engineering

Southern California presents one of the most studied continental margins in the world. Seismic hazards in Southern California have been summarized by the Working Group on California Earthquake Probabilities (1995). Joyner and Boore (1981), Boore (1983), and Kramer (1996) provide correlations for peak horizontal acceleration and frequency of ground motion with respect to earthquake moment magnitude. This work enables one to characterize a hypothetical earthquake. Our algorithm begins by choosing a random earthquake magnitude in the range expected off of Southern California. The distance of the earthquake epicenter from the continental shelf is chosen at random from within a reasonable range of influence that depends on moment magnitude. The depth d at the middle of potential mass failure is then chosen at random subject to several geometric constraints based on typical bathymetry. This depth is the first descriptor of mass failure geometry. The peak horizontal acceleration, frequency of oscillation, and number of cycles are then calculated from earthquake engineering correlations (Kramer, 1996).

3.b Sediment Stability Calculations

Historical sedimentology of the Santa Monica Basin is described by Schwalbach *et al.* (1996) and Gorsline (1996). Schwab et al. (1993) describe the geological context of the Southern California margin and describe several significant mass failure events. These studies provide sediment characteristics and sedimentation rates needed to model sediment response to a nearby earthquake. Earthquake and sediment parameters become inputs in the

sediment failure calculations of Dobry *et al.* (1982), Housner (1985), Kramer (1996), Morgenstern and Price (1965), and Turner and Schuster (1996). We did not consider the effects of sediment grain size distribution, variations and changes in sediment type, seismic and landslide histories, coastal uplift or subsidence, overconsolidation, addition of a recent overburden, artesian water flows, tidal fluctuations, liquefaction, or storm waves in our calculations. For now, quasi-static stability analysis is employed because of its relative simplicity. Several different failure modes are possible for any given sediment. We assume a bulk sediment density of 1900 kg/m^3 throughout this work. Our algorithm randomly chooses a mean yearly sedimentation rate and a reasonable slope inclination. This slope is the second descriptor of mass failure geometry.

The algorithm then splits into sandy/silty sediments and clayey sediments with equal probability. The algorithm chooses a random friction angle, cohesion, and pore water diffusivity suitable for sands and silts. For clays, the algorithm chooses random plasticity and liquidity indices and then calculates shear strength and pore water diffusivity from standard correlations (Bardet, 1997). For both sediment types, sediment is built up based on an instantaneous sedimentation load followed by pore water diffusion for the rest of that year. This enables pore water pressure to accumulate and contribute to failure. Failure occurs when the computed depth of failure matches the current depth of accumulated sediment. We assume that a sufficiently thick sediment blanket exists to accommodate such failure thicknesses. The algorithm randomly chooses the mass failure length according to the sediment type. The mass failure thickness and length complete the description of mass failure geometry. The four geometric variables suffice to calculate the characteristic tsunami amplitude according to (13). The width of mass failure is neglected here, thereby giving maximum possible tsunami amplitudes at generation.

3.c Probability Distributions

Fig. 1 shows the characteristic tsunami amplitude distribution calculated for earthquake epicenters that induce significant ground motion along the continental shelf. The plot provides the per cent less than probability in units of constant standard deviation along the x-axis. The characteristic tsunami amplitude occurs above the underwater landslide or slump. Three-dimensional effects could significantly lower tsunami amplitudes. The mean tsunami amplitude attributed to mass failure is 2.4 meters with a standard deviation of 9.2 meters. Some milestones include 10.5% of earthquakes induced no mass failure, 51.6 % of earthquakes induced tsunamis less than one centimeter in amplitude, and 81.0% of

earthquakes resulted in tsunamis less than one meter in amplitude. The maximum tsunami amplitudes are at least 50 times larger than those expected to be generated by coseismic displacement during earthquakes of similar magnitude with rupture along vertical thrust faults.

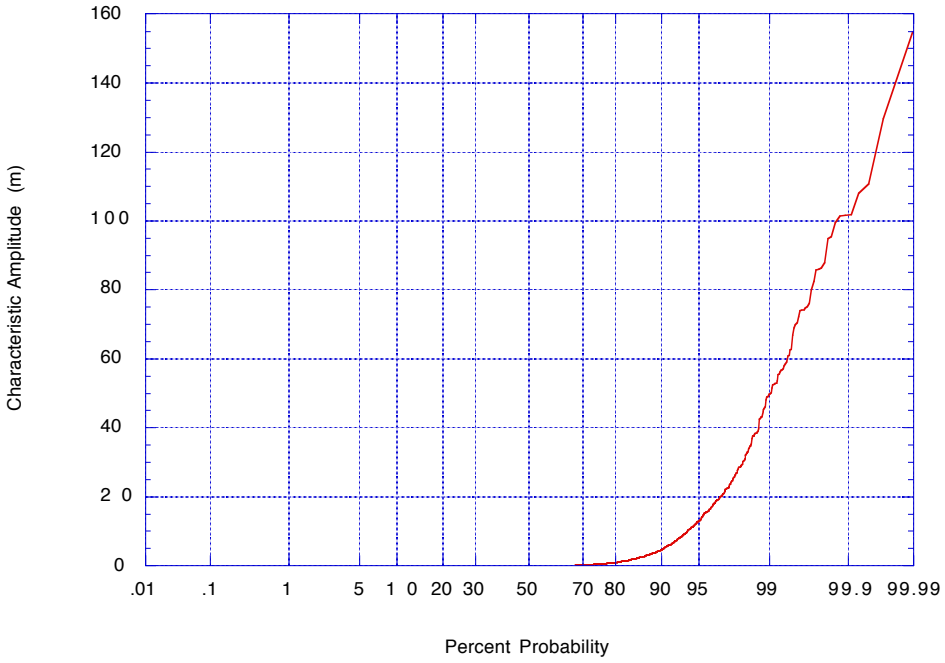

FIGURE 1 Distribution of characteristic tsunami amplitudes.

Fig. 2 displays the probability distribution of mass failure thickness. While there is no simple relation between Figs. 1 and 2, it is safe to say that tsunamigenicity (near the level of one meter in amplitude) begins with mass failure thicknesses greater than around 200 m. This result stems from the minimum mass failure depth of d=500 m chosen for this work and should not be taken out of context. These are realistic mass failure thicknesses. A smaller minimum depth would have resulted in larger tsunamis. Submarine mass failure on the order of 1 km thick is known to have occurred from geological records gathered during marine surveys (Edgers and Karlsrud, 1982; Schwab *et al.*, 1993). Catastrophic tsunamis must occur from time to time.

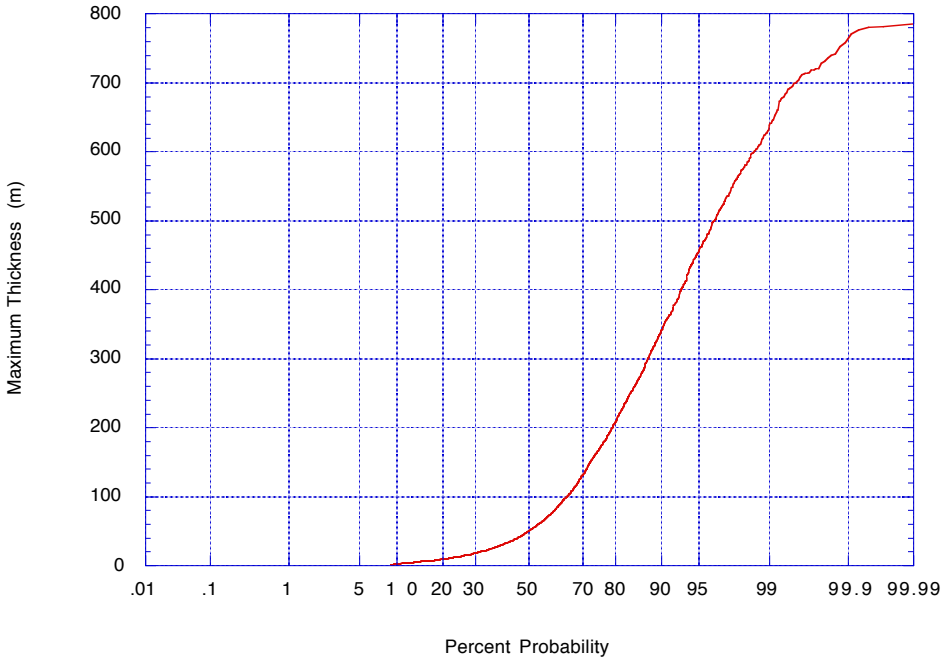

FIGURE 2 Distribution of mass failure thicknesses.

Fig. 3 provides a comparison of the characteristic tsunami amplitude distribution and the observed maximum tsunami runup in the Pacific from 1991-97. These are in fact similar amplitude measures since peak runup from submarine mass failure is often similar to the characteristic tsunami amplitude. The similarities are suggestive of a particular relationship between coseismic displacement and mass failure tsunami generation. Namely, coseismic displacement provides a background tsunami amplitude of several meters onto which submarine mass failure tsunami generation may be contribute much larger peak values. Both mechanisms would act independently since it is possible to have coseismic displacement tsunami generation without mass failure, and mass failure tsunami generation without significant coseismic displacement. Onshore strike-slip faults can trigger submarine mass failure.

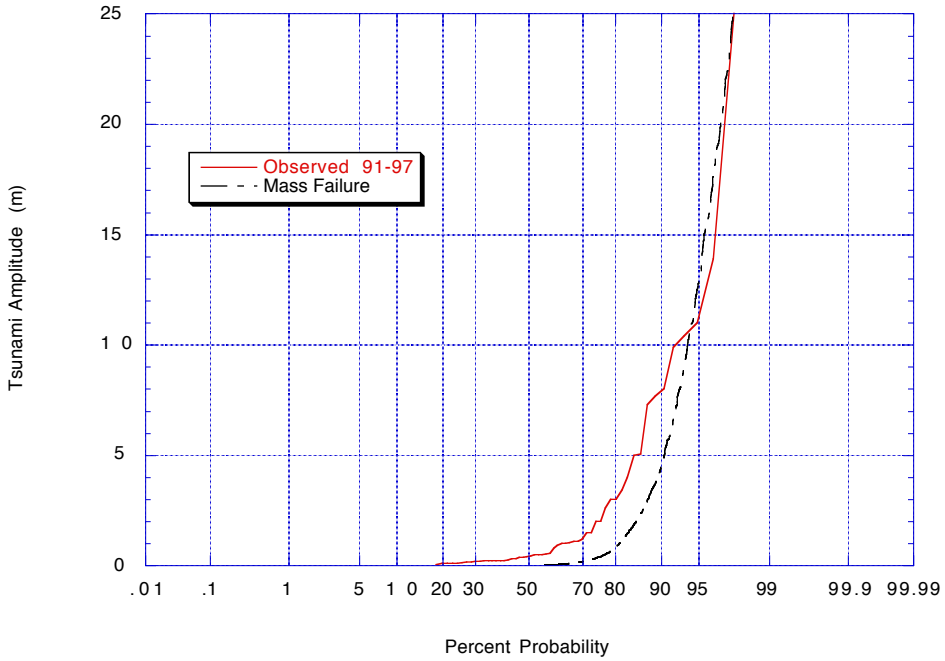

FIGURE 3 Comparison of characteristic amplitude and observed runup distributions.

Fig. 4 demonstrates that large tsunamis can be generated with roughly equal probability by earthquakes with moment magnitudes ranging from 5-7. This result is partly a byproduct of considering only earthquake distances from the margin that can induce failure. For submarine mass movements, tsunami amplitude is largely independent of earthquake magnitude. Enormous tsunamis can be generated by relatively mild earthquakes, significantly lower than the current threshold of $M_W \geq 6.5$ used to issue tsunami watches. Coastal populations may not even feel the earthquake. Hence, education that advises coastal populations to seek high ground whenever the ground shakes may not suffice. A leading depression N-wave may be the most reliable tsunami warning possible.

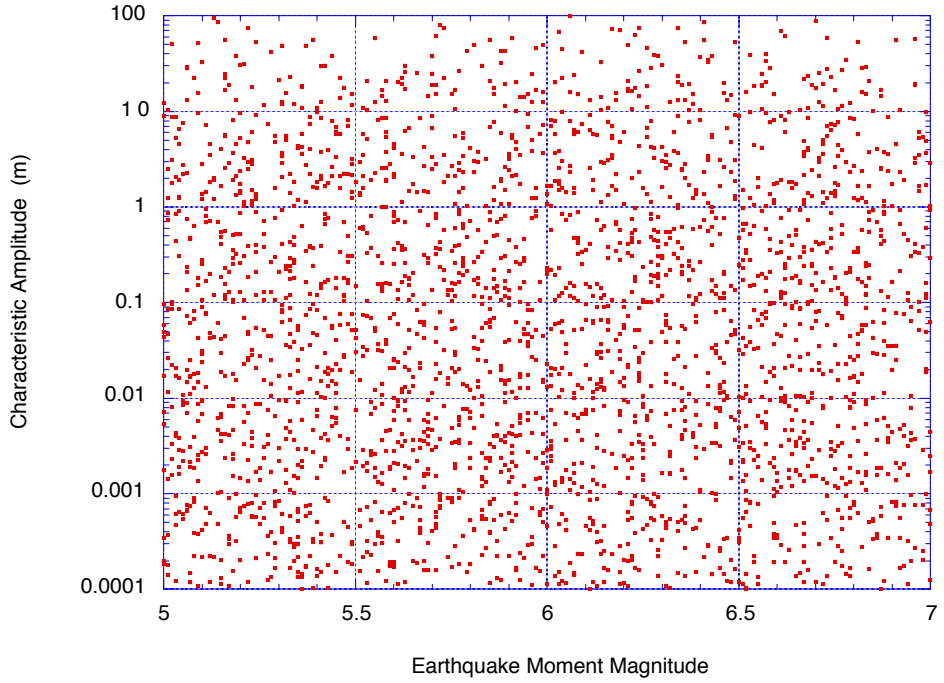

FIGURE 4 Characteristic tsunami amplitude versus earthquake moment magnitude.

Fig. 5, involving only clay simulations, shows that tsunamigenic mass failure occurs in regions of high sediment strength. A low liquidity index is indicative of stiff clay with significant shear strength (Bardet, 1997). The Papua New Guinea tsunami clearly highlights the limitations of the current tsunami warning system as the earthquake was dismissed as having a low probability of generating a destructive local tsunami. In retrospect, given the stiff clays within an offshore region of strong ground motion, a catastrophic tsunami generated by submarine mass failure was a near certainty. Mass failure is more probable in sediments with low strength, although failure tends to be shallow and not tsunamigenic. River deltas offer a case in point (Terzaghi, 1956). We are currently analyzing the sensitivity of tsunami amplitude to all earthquake and sedimentary parameters.

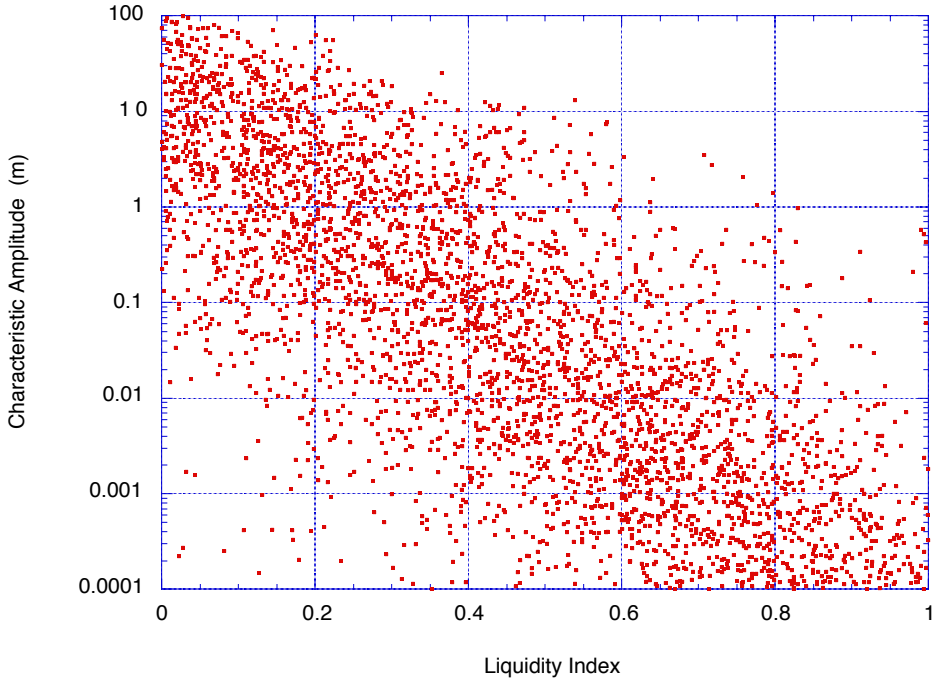

FIGURE 5 Characteristic tsunami amplitude versus earthquake moment magnitude.

4) TSUNAMI WARNING

The preceding algorithm can be evaluated once on a modern personal computer in several seconds. The time is needed to deposit yearly layers of sediment and calculate pore water diffusion. Numerous tsunami generation scenarios can be tested in one minute. Perhaps a reliable prediction of tsunami generation by mass failure can be made. Perhaps submarine mass failure can be detected directly, obviating the need to infer physical processes. In either case, tsunami warnings could be issued for tsunamis generated by submarine mass movement over a limited geographical range. The tsunami hazard assessment provided herein could certainly motivate such efforts.

4.1 Hazards of Mass Failure

The Working Group on California Earthquake Probabilities (1995) places the probability of significant offshore earthquakes at 0.006-0.007 per year. The recurrence interval off of Southern California is therefore once every 15 years over the entire range of earthquake magnitudes considered. A tsunami generated by mass failure with an amplitude greater than 1 m can be expected off of Southern California every 75 years. Historical records indicate two such events in the last two centuries, the 1812 Santa Barbara tsunami and the 1927 Point Arguello tsunami. There has been at least one small mass failure generated tsunami off of California this last decade (Schwab *et al.*, 1993; Gardner-Taggart and Barminski, 1991). In sum, the tsunami amplitude distribution calculated here may actually fit the historical tsunamigenicity off of Southern California. The probability of experiencing a catastrophic event is therefore substantial and may meet the 10% level in 50 years.

4.2 Detection of Mass Failure

Hasegawa and Kanamori (1987) as well as Eissler and Kanamori (1987) show that submarine mass failures produce a distinct monopole distribution of seismic radiation. In addition, recent work on the 1998 Papua New Guinea tsunami shows that the tsunamigenic slump was captured as a low frequency rumbling transmitted by T phases all the way to Wake Island. T phase radiation of submarine mass failure sound can be picked up as ground motion by broadband seismograms located near a shoreline. Local hydrophones can also detect the rumbling associated with mass failure, as can ocean floor mounted broadband seismograms. Only the largest submarine mass failures are readily detected. Hence, tsunami warnings can be issued for tsunamis generated by submarine mass failure.

5) CONCLUSIONS

An estimate of tsunami hazards from submarine mass failure is presented for Southern California. A tsunami exceeding 1 m in amplitude can be expected every 75 years. Maximum tsunami amplitudes may reach approximately 100 m. Sufficient geological and seismic information would enable probability distributions to be calculated for other coastlines. Reliable predictions of tsunamigenic mass failure may be possible soon after a nearshore earthquake. Large mass failure events can be detected, enabling tsunami warnings to be issued. Such warnings can be useful since coastal populations may not feel the triggering earthquake. However, the utility of such warnings in the face of catastrophic tsunami attack is questionable. Most coastal communities are not prepared for catastrophic tsunamis and very little warning time would likely be available to nearby communities. As of now, there is insufficient information on which to base such a hypothetical warning system.

5.1 Acknowledgments

The author is grateful to the organizing committee for partial support to attend the workshop. This work was partially supported by FEMA, with the cooperation of Prof. Costas Synolakis. Mr. Jose Borrero helped code and test the computer program.

6) REFERENCES

Bardet, J.-P. (1997). *Experimental soil mechanics*. Prentice Hall, Upper Saddle River, NJ.

Bjerrum, L. (1971). "Subaqueous slope failures in Norwegian fjords." *Nor. Geotech. Inst. Bull.*, 88, 1-8.

Boore, D. M. (1983). "Stochastic simulation of high-frequency ground motions on seismological models of the radiated spectra." *Bull. Seis. Soc. Am.*, 73(6), 1865-1894.

Cornforth, D. H., and Lowell, J. A. (1996). "The 1994 submarine slope failure at Skagway, Alaska." in *Landslides*, Ed. K. Senneset, 527-532, Balkema, Rotterdam.

Dobry, R., Ladd, R. S., Yokel, F. Y., Chung, R. M., and Powell, D. (1982). *Prediction of pore water pressure buildup and liquefaction of sands during earthquakes by the cyclic strain method*. NBS Building Science Series 138, Nat. Bureau Standards, U.S., Dept. of Commerce, Washington, D.C.

Edgers, L., and Karlsrud, K. (1982). "Soil flows generated by submarine slides: case studies and consequences." *Nor. Geotech. Inst. Bull.*, 143, 1-11.

Eissler, H. K., and Kanamori, H. (1987). "A single-force model for the 1975 Kalapana, Hawaii, earthquake." *J. Geophys. Res.*, 92(B6), 4827-4836.

Gardner-Taggart, J. M., and Barminski, R. F. (1991). "Short period wave generation in Moss Landing harbor caused by offshore landslides induced by the Loma Prieta earthquake." *Geophys. Res. Letters*, 18(7), 1277-1280.

Geist, E. L. (1998). "Local tsunamis and earthquake source parameters." *Adv. in Geophys.*, 39, 117-209.

Gorsline, D. S. (1996). "Depositional events in Santa Monica Basin, California Borderland, over the past five centuries." *Sed. Geol.*, 104, 73-88.

Grilli, S. T., Skourup, J., and Svendsen, I. A. (1989). "An efficient boundary element method for nonlinear water waves." *Engrg. Analysis with Boundary Elements*, 6(2), 97-107.

Grilli, S. T., and Svendsen, I. A. (1990). "Corner problems and global accuracy in the boundary element solution of nonlinear wave flows." *Engrg. Analysis with Boundary Elements*, 7(4), 178-195.

Grilli, S. T., and Subramanya, R. (1994). "Quasi-singular integrals in the modeling of nonlinear water waves in shallow water." *Engrg. Analysis with Boundary Elements*, 13, 181-191.

Grilli, S. T., and Subramanya, R. (1996). "Numerical modeling of wave breaking induced by fixed or moving boundaries." *Comp. Mech.*, 17, 374-391.

Grilli, S. T., and Watts, P. (1999). "Modeling of waves generated by a moving submerged body: Applications to underwater landslides." *Engrg. Analysis with Boundary Elements*, 23(8), 645-656.

Hammack, J. L. (1973). "A note on tsunamis: Their generation and propagation in an ocean of uniform depth." *J. Fluid Mech.*, 60, 769-799.

Hampton, M. A., Lee, H. J., and Locat, J. (1996). "Submarine landslides." *Rev. Geophys.*, 34(1), 33-59.

Hasegawa, H. S., and Kanamori, H. (1987). "Source mechanism of the magnitude 7.2 Grand Banks earthquake of November 1929: Double couple or submarine landslide?" *Bull. Seis. Soc. Am.*, 77(6), 1984-2004.

Housner, G. W. (1985). *Liquefaction of soils during earthquakes*. National Academy Press, Washington, D.C.

Imamura, F., and Gica, E. C. (1996). "Numerical model for tsunami generation due to subaqueous landslide along a coast." *Sci. Tsunami Hazards*, 14, 13-28.

Joyner, W. B., and Boore, D. M. (1981). "Peak horizontal acceleration and velocity from strong-motion records including records from the 1979 Imperial Valley, California earthquake." *Bull. Seis. Soc. Am.*, 71(6), 2011-2038.

Kramer, S. L. (1996). *Geotechnical earthquake engineering*. Prentice Hall, Upper Saddle River, NJ.

Lee, H. J., and Edwards, B. D. (1986). "Regional method to assess offshore slope stability." *J. Geotech. Engrg.*, ASCE, 112(5), 489-509.

Morgenstern, N. R., and Price, V. E. (1965). "The analysis of the stability of general slip surfaces." *Geotechnique*, 15, 79-93.

Nayfeh, A. H., and Mook, D. T. (1979). *Nonlinear oscillations*. Wiley-Interscience, New York, N.Y.

Pelinovsky, E., and Poplavsky, A. (1996). "Simplified model of tsunami generation by submarine landslide." *Phys. Chem. Earth*, 21(12), 13-17.

Plafker, G., Kachadoorian, R., Eckel, E. B., and Mayo, L. R. (1969). "The Alaska earthquake March 27, 1964: Various communities." U.S. Geol. Surv. Prof. Paper 542-G, U.S., Dept. of Interior, Washington, D.C.

Prior, D. B., and Coleman, J. M. (1979). "Submarine landslides: Geometry and nomenclature." *Z. Geomorph. N. F.*, 23(4), 415-426.

Sarpkaya, T., and Isaacson, M. (1981). *Mechanics of wave forces on offshore structures*. Van Nostrand Reinhold, New York, N.Y.

Schwab, W. C., Lee, H. J., Twichell, D. C. (1993). Submarine landslides: Selected studies in teh U.S. exclusive economic zone. U.S. Geol. Surv. Bull. 2002, U.S., Dept. of Interior, Washington, D.C.

Schwalbach, J. R., Edwards, B. D., and Gorsline, D. S. (1996). "Contemporary channel-levee systems in active borderland basin plains, California Continental borderland." *Sed. Geol.*, 104, 53-72.

Seed, H. B., Seed, R. B., Schlosser, F., Blondeau, F., and Juran, I. (1988). "The landslide at the Port of Nice on October 16, 1979." *Rep. No. UCB/EERC-88/10*, Earthquake Engineering Research Center, University of California, Berkeley, CA.

Tadepalli, S., and Synolakis, C. E. (1994). "The run-up of N-waves on sloping beaches." *Proc. R. Soc. Lond. A*, 445, 99-112.

Tadepalli, S., and Synolakis, C. E. (1996). "Model for the leading waves of tsunamis." *Phys. Rev. Letters*, 77(10), 2141-2144.

Tappin, D. R., Matsumoto, T., and shipboard scientists. (1999). "Offshore geological investigation of the July 1998 Sissano tsunami, Papua new Guinea." *EOS, Trans. Am. Geophys. Union*, 80(30), 329.

Terzaghi, K. (1956). "Varieties of submarine slope failures." *Proc. 8th Texas Conf. Soil Mech. Found. Eng.*, 1-41.

Turner, A. K., and Schuster, R. L. (1996). *Landslides: Investigation and mitigation*. Special Report 247, Trans. Res. Board, National Academy Press, Washington, D.C.

Watts, P. (1998). "Wavemaker curves for tsunamis generated by underwater landslides." *J. Wtrwy, Port, Coast, and Oc. Engrg.*, ASCE, 124(3), 127-137.

Watts, P. (2000). "Tsunami features of solid block underwater landslides." *J. Wtrwy, Port, Coast, and Oc. Engrg.*, ASCE, in press.

Working Group on California Earthquake Probabilities (1995). "Seismic hazards in Southern California: Probable earthquakes, 1994 to 2024." *Bull. Seis. Soc. Am.*, 85(2), 379-439.